



ELSEVIER

Journal of Luminescence 75 (1997) 221–227

JOURNAL OF  
LUMINESCENCE

# Infrared to green up-conversion in $\text{LaCl}_3:\text{U}^{3+}$

M. Yin<sup>a,b,\*</sup>, M.-F. Joubert<sup>c</sup>, J.-C. Krupa<sup>b</sup><sup>a</sup>Department of Physics, University of Science and Technology of China, 230026 Hefei, China<sup>b</sup>Groupe de Radiochimie, Institut de Physique Nucleaire, CNRS-IN2P3, B.P. 1, 91406 Orsay Cedex, France<sup>c</sup>Laboratoire de Physico-Chimie des Matériaux Luminescents, Université Claude Bernard Lyon 1, UMR CNRS 5620, 43, bd du 11 novembre 1918, bat. 205, 69622 Villeurbanne Cedex, France

Received 21 January 1997; accepted 9 June 1997

## Abstract

Investigations of the optical properties of  $\text{LaCl}_3:\text{U}^{3+}$  (0.1%) single crystal have revealed an interesting up-conversion phenomenon. When the  ${}^4\text{G}_{7/2}$  level of  $\text{U}^{3+}$  is excited by an infrared laser set at 748.6 nm, a strong green fluorescence from the  ${}^2\text{K}_{15/2}$  level is observed. From the analysis of the dynamics of the excited states, we conclude that the observed phenomenon occurs mainly via two mechanisms: (i) excited-state absorption and (ii) an energy transfer up-conversion (ETU) process involving pairs of  $\text{U}^{3+}$  ions in  ${}^4\text{G}_{5/2}$  and  ${}^4\text{F}_{9/2}$  states.

PACS: 78.55; 78.30; 42.70

Keywords: Up-conversion mechanism; Low-temperature photoluminescence spectra;  $\text{LaCl}_3:\text{U}^{3+}$ 

## 1. Introduction

Up-conversion mechanisms are again being widely investigated at present. This renewed interest is related to the available low-cost infrared excitation sources opening a new world for display devices and the appearance of up-conversion-pumped solid-state lasers. Efficient up-conversion is possible in rare-earth or actinide-doped materials with metastable, intermediate levels that can act as a storage reservoir for pump energy. The anti-Stokes emission may happen by several types of up-conversion processes: excited-state absorption (ESA) first proposed by Bloembergen for IR quantum counters [1], ETU discovered by Auzel [2],

cooperative sensitization [3] or cooperative luminescence [4].

$\text{LaCl}_3$  is a very good host for luminescent materials. Spectra and energy levels of all rare earth and actinide ions in the crystal have been studied extensively [5, 6]. There are many publications on up-conversion phenomenon in  $\text{LaCl}_3:\text{RE}$  (RE = trivalent rare-earth ions) [7–9] and  $\text{LaCl}_3:\text{Pr}^{3+}$  is thought to be one of the most efficient up-conversion laser systems [10] which operates up to 210 K. However, similar reports for actinide-doped  $\text{LaCl}_3$  are very few. We present here infrared to green up-conversion in  $\text{LaCl}_3:\text{U}^{3+}$ . The experimental results are interpreted using a rate-equation analysis.

## 2. Experimental procedure and results

All data presented here were taken using  $\text{LaCl}_3:\text{U}^{3+}$  of nominally 0.1 mol% concentration

\* Correspondence address: Groupe de Radio chimie, Institut de Physique Nucleaire, Université de Paris. CNRS-IN2P3, B.P.1, 91406 orsay Cedex, France. Tel.:33169157345; Fax: 33169156470; e-mail: yinmin@phys.ustc.edu.cn.

mounted in a quartz tube under a partial pressure of He gas and set in a circulating He cryostat held at 8 K. In all cases, excitation was provided by pulsed radiation (during 10 ns) from a dye laser pumped by a frequency-doubled (tripled) YAG:Nd<sup>3+</sup> laser. Fluorescence from the sample was collected into a HRS2 Jobin–Yvon monochromator and detected with either a R1767 or a R943-02 Hamamatsu photomultiplier tube depending on spectrum range. The decay-time measurements were realized using a Lecroy 9410 oscilloscope interfaced with a computer. The dyes used in this work are Coumarin 500, DCM and LDS751.

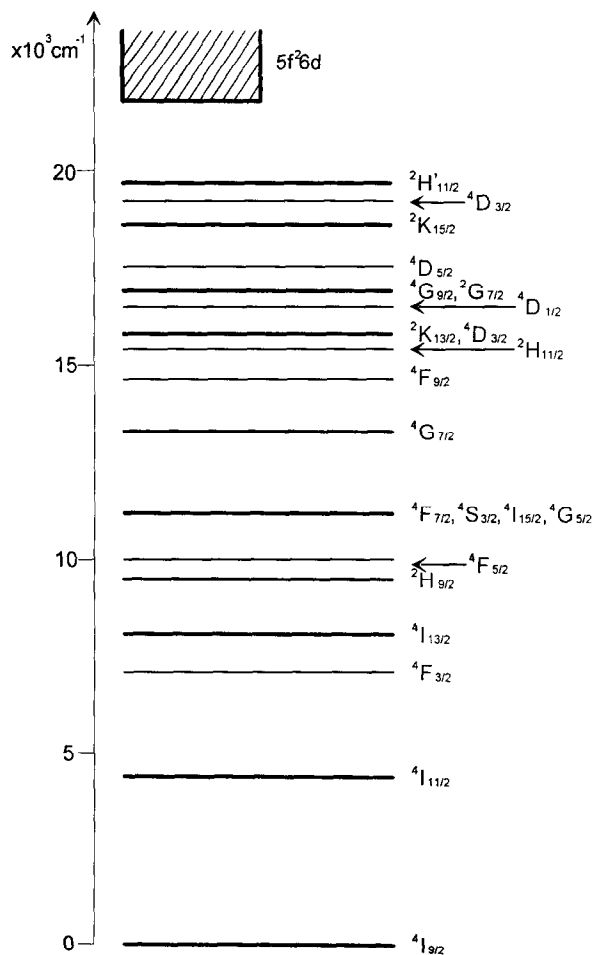


Fig. 1. Energy level diagram of U<sup>3+</sup> in LaCl<sub>3</sub>.

The energy level scheme of U<sup>3+</sup> ions in LaCl<sub>3</sub>, following the results of Refs. [6, 11], is shown in Fig. 1. After pumping at 748.6 nm in one of the <sup>4</sup>G<sub>7/2</sub> Stark levels, we observed an intense green (around 550 nm) fluorescence from the <sup>2</sup>K<sub>15/2</sub> level which lies more than 5000 cm<sup>-1</sup> above the <sup>4</sup>G<sub>7/2</sub> level. Weak up-converted fluorescence from <sup>2</sup>H<sub>11/2</sub> level was also observed around 515 nm. The corresponding emission spectrum is plotted in Fig. 2a. As there is no emission from <sup>2</sup>K<sub>15/2</sub> level at room temperature, which is mainly due to the increase of non-radiative transition probability, the experimental temperature was kept at 8 K.

In order to study the time-dependent behavior of the system, several transients were recorded. The decay of the fluorescence from <sup>4</sup>G<sub>7/2</sub> is exponential after selective excitation into this manifold and the lifetime is equal to 0.56 μs (see Table 1). Always after selective pumping at 748.6 nm, decays were recorded for the 552 nm green fluorescence from <sup>2</sup>K<sub>15/2</sub> (Fig. 2a), as well as the 988 nm infrared emission from <sup>4</sup>F<sub>9/2</sub> (Fig. 2b) and the 923 nm emission from <sup>4</sup>G<sub>5/2</sub> (Fig. 2b). Fig. 3 shows these experimental decays together with the fitting results using the model discussed below.

### 3. Discussion

To get information concerning the up-conversion process responsible for such a green fluorescence, it is necessary to analyze the shape of its decay which is plotted in Fig. 3a. At short times, it exhibits first a very steep decay with a time constant of approximately 0.1 μs which is followed by a rising slope to a second maximum (rise time ~1 μs) and finally a decay with a time constant of 4.1 μs. This decay curve indicates that there are at least two mechanisms responsible for the up-conversion fluorescence, corresponding to the two parts of the decay curve, named part 1 and 2, respectively.

Let us consider first the fast-decay part (part 1). The absence of an initial rise time and the fact that this anti-Stokes fluorescence decay ( $\tau = 0.1 \mu\text{s}$ ) characterizes the upper emitting level (see Table 1) suggest that the mechanism responsible for this emission is an ESA process. After laser excitation

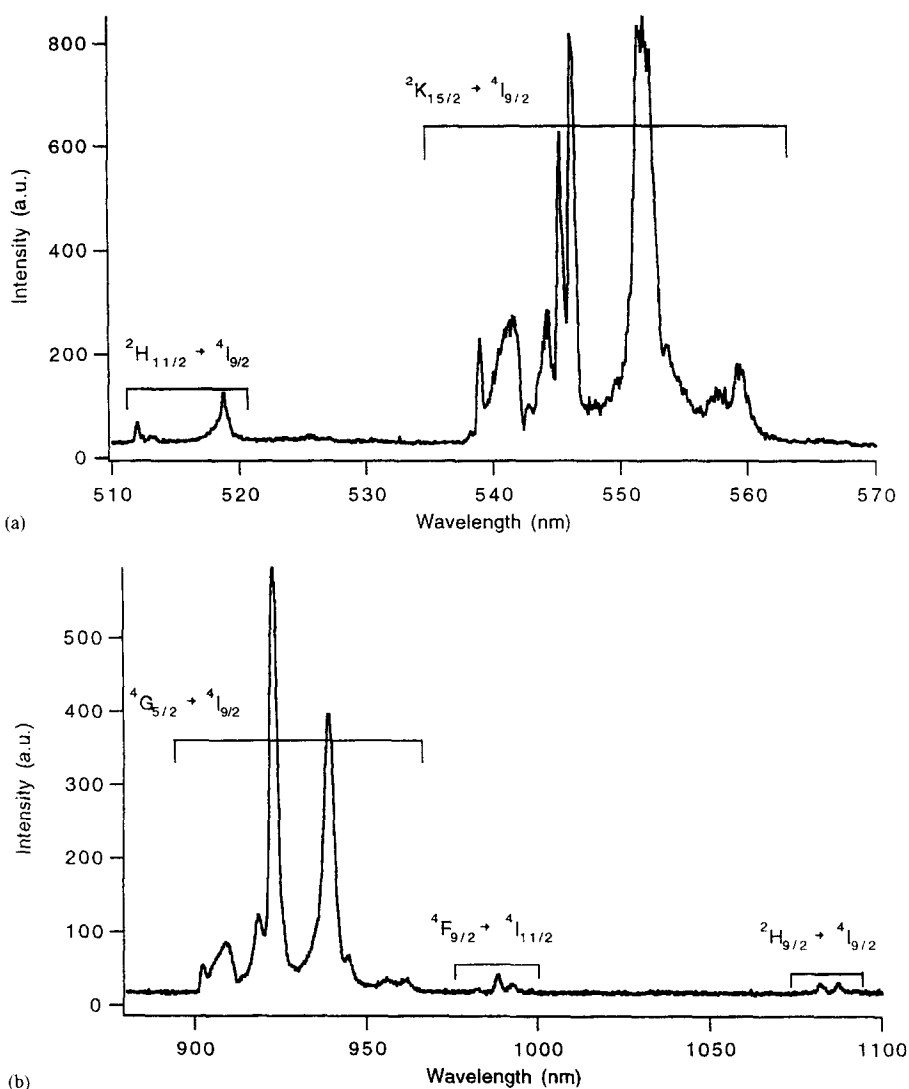


Fig. 2. Fluorescence spectra of  $\text{LaCl}_3:\text{U}^{3+}$  (0.1%) under 748.6 nm dye-laser excitation at 8 K. (a) up-converted green emission (510–570 nm); (b) infrared emission (880–1100 nm).

Table 1

Lifetimes of main fluorescing levels of  $\text{U}^{3+}$  in  $\text{LaCl}_3:0.1\%\text{U}^{3+}$  at 8 K. Except the  ${}^4I_{11/2} \rightarrow {}^4I_{9/2}$  fluorescence which was analyzed after excitation in  ${}^4F_{3/2}$ , the decay curves have been recorded after selective excitation in the emitting level

Energy level	${}^2K_{15/2}$	${}^2H_{11/2}$	${}^4F_{9/2}$	${}^4G_{7/2}$	${}^4G_{5/2}$	${}^4F_{3/2}$	${}^4I_{11/2}$
Lifetime( $\mu\text{s}$ )	~0.1	2.5	14	0.56	6.1	130	770

into the  ${}^4G_{7/2}$  state, new incoming photons are again absorbed by  $\text{U}^{3+}$  in this excited state in order to populate levels belonging to the  $5f^26d$  excited configuration which lies in this energy range (see Fig. 1). From there the lower states  ${}^2H'_{11/2}$  and  ${}^2K_{15/2}$  are populated by a rapid phonon relaxation and then the radiative transitions from  ${}^2H'_{11/2}$  and  ${}^2K_{15/2}$  to  ${}^4I_{9/2}$  take place. Therefore, part 1 of the

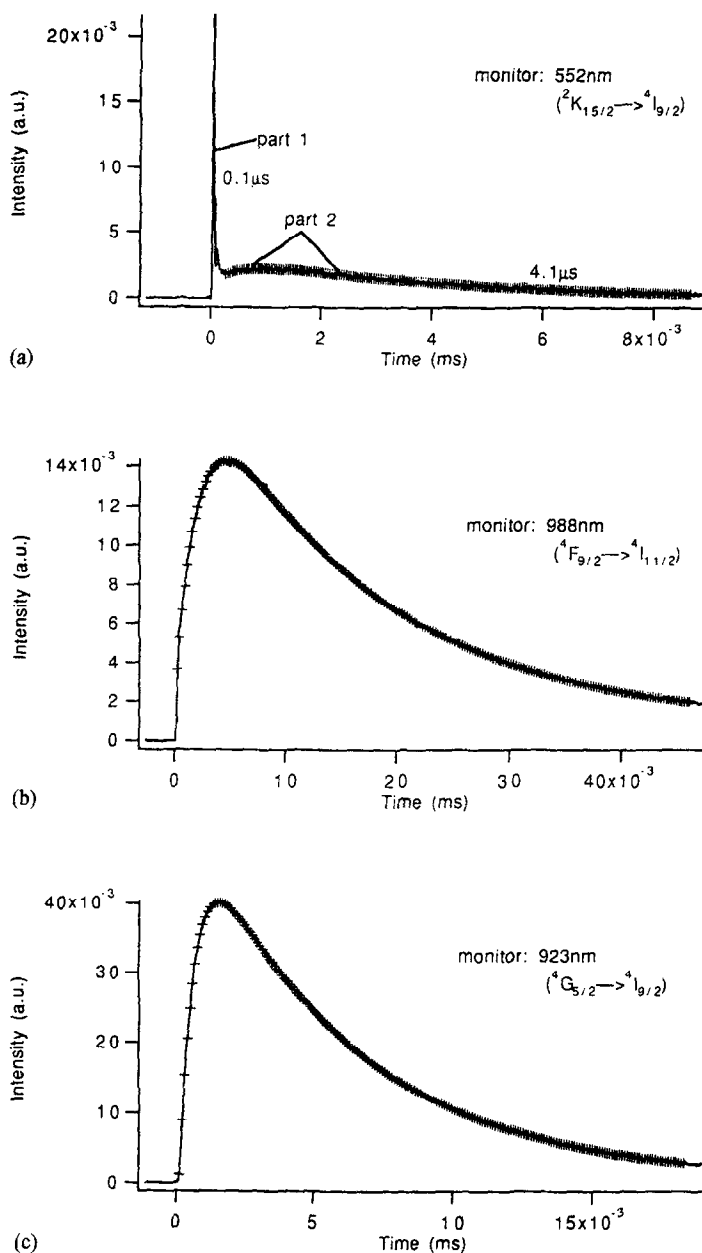
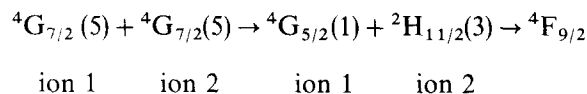


Fig. 3. Experimental decay curves for different transitions under 748.6 nm excitation at 8 k: (a)  ${}^2K_{15/2} \rightarrow {}^4I_{9/2}$ ; (b)  ${}^4F_{9/2} \rightarrow {}^4I_{11/2}$ ; (c)  ${}^4G_{5/2} \rightarrow {}^4I_{9/2}$  and fitting results denoted by “+ line”.

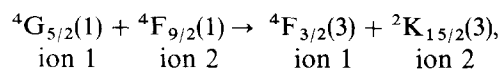
552 nm fluorescence time dependence corresponds to the decay of  ${}^2K_{15/2}$  level populated via an excited state absorption process through highly allowed  $5f^3 \rightarrow 5f^2 6d$  transitions.

The slowest part of Fig. 3a (part 2) suggests that metastable  $5f^3$  levels with a few  $\mu\text{s}$  lifetimes are probably involved in an up-conversion process populating  ${}^2K_{15/2}$ . We know that  ${}^4G_{5/2}$  has a

lifetime of 6.1  $\mu\text{s}$  (Table 1). After selective excitation into  ${}^4\text{G}_{7/2}$ , we observed an intense emission from  ${}^4\text{G}_{5/2}$  around 930 nm (see Fig. 2b). The time behavior of the most intense line at 923 nm, plotted in Fig. 3c, shows an exponential rise followed by an exponential decay with fitting time constants of 0.56 and 6.1  $\mu\text{s}$ , respectively. This indicates that  ${}^4\text{G}_{5/2}$  is populated via  ${}^4\text{G}_{7/2}$  single-ion relaxation. The  ${}^4\text{F}_{9/2}$  manifold located just above  ${}^4\text{G}_{7/2}$  has a lifetime of 14  $\mu\text{s}$  (Table 1). After selective excitation into  ${}^4\text{G}_{7/2}$ , fluorescence related to the  ${}^4\text{F}_{9/2} \rightarrow {}^4\text{I}_{11/2}$  transition is identified in Fig. 2b, and the time behavior of the line at 988 nm, plotted in Fig. 3b, shows a rise of a few  $\mu\text{s}$  followed by an exponential decay with a time constant of 14  $\mu\text{s}$ . Fitting result gives  $\tau_{\text{rise}} = 2 \mu\text{s}$ . The energy-level structure and lifetime of  $\text{LaCl}_3:\text{U}^{3+}$  suggest that the  ${}^4\text{F}_{9/2}$  manifold may be populated by the following process.



(numbers in parentheses are twice the value of the crystal-field quantum numbers  $\mu$ ). This also explains why  ${}^4\text{G}_{7/2}$  level has a larger energy gap but possesses a shorter lifetime compared with  ${}^4\text{F}_{9/2}$ . In order to interpret the  ${}^2\text{K}_{15/2} \rightarrow {}^4\text{I}_{9/2}$  fluorescence decay curves, we propose the model schematized in Fig. 4. This model takes into account the efficient excited-state absorption described in the beginning of this section and the following cross relaxation energy transfer:



for which the energy mismatch of  $29 \text{ cm}^{-1}$  can be easily absorbed by the lattice vibrations. For this cross-relaxation process, ion 1 is initially in the  ${}^4\text{G}_{5/2}$  state due to one-ion relaxation from  ${}^4\text{G}_{7/2}$  and ion 2 is initially in the  ${}^4\text{F}_{9/2}$  state due to the ESA already mentioned followed by one-ion relaxation. This model leads, just after the excitation pulse, to the following rate equation system A, where  $n_i$  is the level  $i$  population,  $k_i$  is the inverse of the level  $i$  lifetime,  $k_{ij}$  is the relaxation rate from level  $i$  to level  $j$  and  $k_0$  is the cross-relaxation

transfer rate:

$$\text{system A} \quad \begin{cases} \frac{dn_1}{dt} = k_{21}n_2 - k_1n_1 - k_0n_1n_3, \\ \frac{dn_2}{dt} = -k_2n_2, \\ \frac{dn_3}{dt} = k_{43}n_4 - k_3n_3 - k_0n_1n_3, \\ \frac{dn_4}{dt} = k_{54}n_5 - k_4n_4, \\ \frac{dn_5}{dt} = -k_5n_5 + k_0n_1n_3. \end{cases}$$

The ETU process has a quite low efficiency because it does not change the decay time of the  ${}^4\text{G}_{5/2}$  and  ${}^4\text{F}_{9/2}$  manifolds which are 6.1 and 14  $\mu\text{s}$ , respectively (see Fig. 3c and Fig. 3b). So we may neglect the term  $k_0n_1n_3$  in the first and third equations of system A. (In fact, in writing system A we already used the similar consideration to simplify the problem.) Moreover, due to this low efficiency of the ETU process and as the  ${}^2\text{K}_{15/2}$  lifetime is much shorter than the  ${}^2\text{H}_{11/2}$  lifetime (see Table 1), we may neglect the term  $k_{54}n_5$  to fit the expressions of the populations in the  $\mu\text{s}$  time range. These approximations lead to

system B

$$\begin{cases} n_1(t) = \frac{n_2(0)k_{21}}{k_2 - k_1} [\exp(-k_1t) - \exp(-k_2t)], \\ n_2(t) = n_2(0) \exp(-k_2t), \\ n_3(t) \approx \frac{n_4(0)k_{43}}{k_4 - k_3} [\exp(-k_3t) - \exp(-k_4t)], \\ n_4(t) \approx n_4(0) \exp(-k_4t), \\ n_5 \approx \left[ n_5(0) - \frac{k_0n_2(0)n_4(0)k_{21}k_{43}}{k_5(k_2 - k_1)(k_4 - k_3)} \right] \\ \times \exp(-k_5t) + \frac{k_0n_2(0)n_4(0)k_{21}k_{43}}{k_5(k_2 - k_1)(k_4 - k_3)} \\ \times [\exp(-(k_1 + k_3)t) + \exp(-(k_2 + k_4)t) \\ - \exp(-(k_2 + k_3)t) - \exp(-(k_1 + k_4)t)]. \end{cases}$$

If we set  $((k_0n_2(0)n_4(0)k_{21}k_{43})/(k_5(k_2 - k_1)(k_4 - k_3))) = w_0$  and consider the big difference of lifetimes (Table 1), the expression of  $n_5(t)$  can

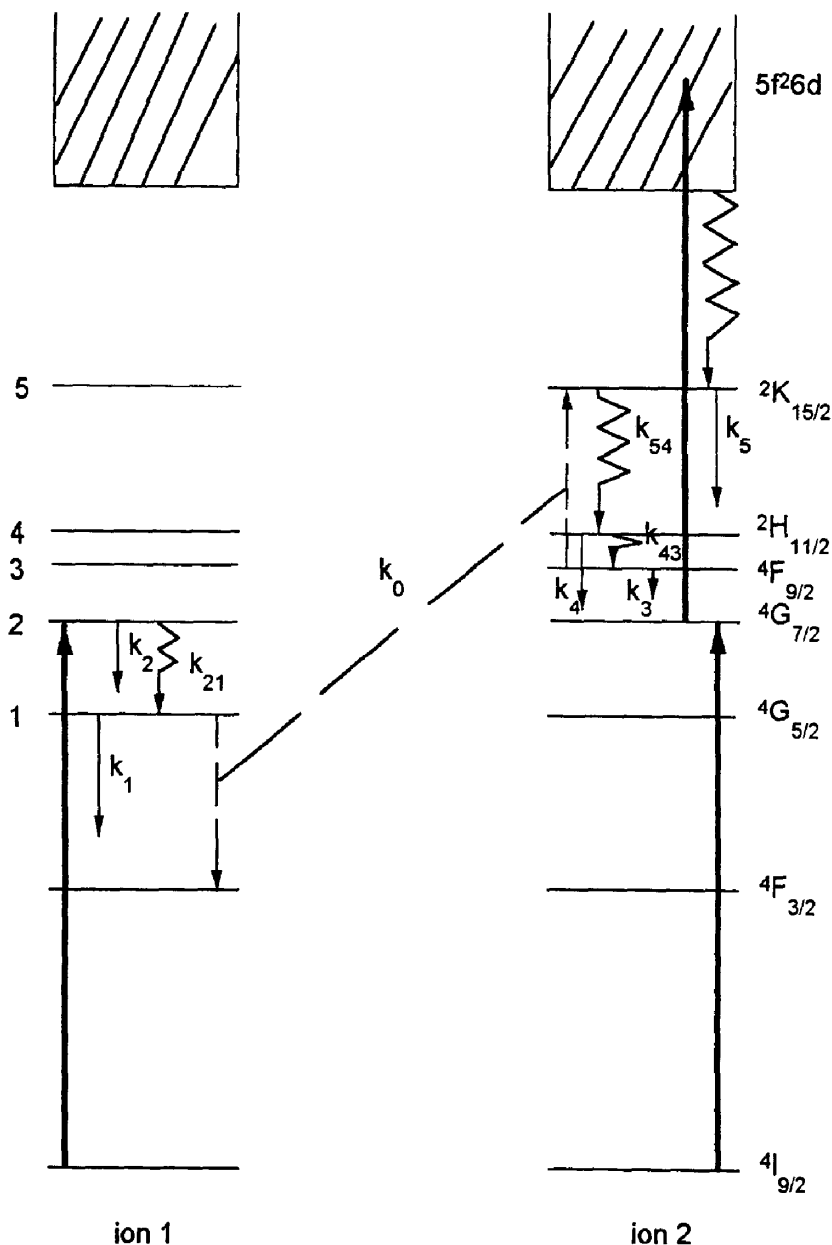


Fig. 4. Scheme for the proposed model. Thick lines represent transitions induced by the radiation field, thin lines represent single-ion relaxation rates and the dashed lines represent transitions induced by inter-ionic coupling. For simplicity, only the related levels are given here.

be simplified as

$$n_5 \approx [n_5(0) - w_0] \exp(-k_5 t) + w_0 \times [\exp(-(k_1 + k_3)t) - \exp(-(k_1 + k_4)t)].$$

It shows that under excitation to  $4G_{7/2}$ , the decay of  $2K_{15/2}$  fluorescence consists of two parts: a one-exponential process with time constant of  $1/k_5 = 0.1 \mu s$  (part 1) followed by a two-exponential

process (part 2), in which, the first part matches the experimental result. The best fit of the second part of the experimental transient gives  $\tau_{\text{rise}} = 0.52 \mu\text{s}$  and  $\tau_{\text{decay}} = 4.1 \mu\text{s}$ . The constant  $4.1 \mu\text{s}$  just equals to  $1/k_1 + k_3 = 4.2 \mu\text{s}$  predicted by the model while  $0.52 \mu\text{s}$  is smaller than the predicted value  $1/k_1 + k_4 = 1.8 \mu\text{s}$ . This difference may indicate that other energy-transfer mechanisms are also possible in the up-conversion process where many levels could be involved.

It should be pointed out that the transient for up-conversion emission  ${}^2\text{H}_{11/2} \rightarrow {}^4\text{I}_{9/2}$  (Fig. 2a) does not show any second component, which is consistent with our model.

#### 4. Conclusions

We have observed a green up-conversion fluorescence from the  ${}^2\text{K}_{15/2}$  level under infrared pumping. The dynamics of the up-converted emission indicates that excited-state absorption from the  ${}^4\text{G}_{7/2}$  level and energy transfer up-conversion process involving pairs of ions in  ${}^4\text{G}_{5/2}$  and  ${}^4\text{F}_{9/2}$  states are responsible for the phenomenon. A simple rate

equation modeling is very successful in reproducing the emission decay time.

#### References

- [1] N. Bloembergen, Phys. Rev. Lett. 2 (1959) 84.
- [2] F. Auzel, C.R. Acad. Sci. (Paris) 262 (1966) 1016.
- [3] V.V. Ovsyankin, P.P. Feofilov, Sov. Phys. JETP Lett. 4 (1966) 317.
- [4] E. Nakazawa, S. Shionoya, Phys. Rev. Lett. 25 (1970) 1710.
- [5] G.H. Dieke, in: Spectra and Energy Levels of Rare Earth Ions in Crystals, H.M. Crosswhite, H. Crosswhite (Eds.), Spectra and Energy Levels of Rare Earth ions in Crystals, Interscience, New York, 1968.
- [6] W.T. Carnall, A Systematic Analysis of the Spectra of Trivalent Actinide Chlorides in  $\text{D}_{3h}$  Site Symmetry. ANL-89/39.
- [7] J.C. Wright, D.J. Zalucha, H.V. Lauer, D.E. Cox, F.K. Fong, J. appl. Phys. 44 (1973) 781.
- [8] D.J. Zalucha, J.A. Sell, F.K. Fong, J. Chem. Phys. 60 (1974) 1660.
- [9] M.E. Koch, A.W. Kueny, W.E. Case, Appl. Phys. Lett. 56 (1990) 1083.
- [10] M.F. Joubert, S. Guy, B. Jacquier, C. Linares, Opt. Mater. 4 (1) (1994) 43.
- [11] H.M. Crosswhite, H. Crosswhite, W.T. Carnall, A.P. Paszek, J. Chem. Phys. 72 (1980) 5103.